SPECTROSCOPIC ORBITS OF SUBSYSTEMS IN MULTIPLE STARS. V.

Andrei Tokovinin
Cerro Tololo Inter-American Observatory, Casilla 603, La Serena, Chile
Draft version January 2, 2019

ABSTRACT

Spectroscopic orbits are determined for inner subsystems in nine stellar hierachies (HIP 2863, 4974, 8353, 28796, 35261, 92929, 115272, 115552, and 117596). Their periods range from 2.5 to 312 days. For each system, estimates of masses, orbital inclination and other parameters are given.

Subject headings: binaries:spectroscopic, binaries:visual

1. INTRODUCTION

Spectroscopic orbits of nine close binaries belonging to hierarchical stellar systems are determined here, continuing the series of similar papers (Tokovinin 2016a,b, 2018b,c). Knowledge of orbital periods and other characteristics of hierarchical systems paves the way to constrain and refine theories of their formation, still in their infancy. Binaries with periods on the order of a few days, studied here, are affected by tides, and the distribution of their periods is expected to reflect the role of tidal interaction in the formation of inner subsystems. The current collection of data on stellar hierarchies (Tokovinin 2018a) contains many spectroscopic binaries with yet unknown orbits. Ongoing work slowly fills this gap.

The systems studied here are listed in Table 1. The data are collected from Simbad and *Gaia* DR2 (Gaia collaboration 2018), the radial velocities (RVs) are mostly determined here. The first column gives the WDS-style (Mason et al. 2001) code based on the J2000 coordinates (all objects are actually present in the WDS).

The structure of this paper is similar to the previous ones. The data and methods are briefly recalled in Section 2, where the orbital elements are also given. Then each system is discussed in Section 3. The paper closes with a short summary in Section 4.

2. OBSERVATIONS AND DATA ANALYSIS

2.1. *Spectroscopic observations*

The spectra used here were taken with the 1.5 m telescope sited at the Cerro Tololo Inter-American Observatory (CTIO) in Chile and operated by the SMARTS Consortium.[1] The observing time was allocated through NOAO. Observations were made with the CHIRON optical echelle spectrograph (Tokovinin et al. 2013) by the telescope operators in service mode. The RVs are determined from the cross-correlation function (CCF) of echelle orders with the binary mask based on the solar spectrum, as detailed in (Tokovinin 2016a). The RVs derived by this method should be on the absolute scale if the wavelength calibration is accurate. The CHIRON RVs were checked against standards and a small offset of $+0.15$ km s^{-1} was found in Tokovinin (2018b); it is not applied to the RVs given here.

The CCF contains two dips in the case of double-lined systems. The dip width is related to the projected rotation speed $V \sin i$, while its area depends on the spectral type, metallicity, and relative flux. Table 2 lists average parameters of the Gaussian curves fitted to the CCF dips. It gives the number of averaged measurements N (blended CCFs were not used), the dip amplitude a, its dispersion σ, the product $a\sigma$ proportional to the dip area (hence to the relative flux), and the projected rotation velocity $V \sin i$, estimated from σ by the approximate formula given in (Tokovinin 2016a) and valid for $\sigma < 12$ km s^{-1}. The last column indicates the presence or absence of the lithium 6708Å line in individual components.

2.2. *Orbit calculation*

As in the previous papers of this series, orbital elements and their errors were determined by the least-squares fits with weights inversely proportional to the adopted errors. The IDL code `orbit`[2] was used (Tokovinin 2016c). It can fit spectroscopic, visual, or combined visual/spectroscopic orbits. Formal errors of orbital elements are determined from these fits. The elements of spectroscopic orbits are given in Table 3, in standard notation. Its last column contains the masses $M \sin^3 i$ for double-lined binaries. For single-lined systems, the mass of the primary star (listed here with colons) is estimated from its absolute V magnitudes, and the minimum mass of the secondary that corresponds to the 90° inclination is derived from the orbit. Table 4, published in full electronically, provides individual RVs. The HIP number and the system identifier (components joined by comma) in the first two columns define the pair. Then follow the Julian date, the RV, its adopted error σ (blended CCF dips are assigned large errors), and the residual to the orbit (O−C). The last column specifies to which component this RV refers ('a' for the primary and 'b' for the secondary). The RVs of other visual components are provided, for completeness, in Table 5. It contains the HIP number, the component letter, the Julian date, and the RV.

3. INDIVIDUAL OBJECTS

For each observed system, the corresponding Figure shows a typical CCF (the Julian date and individual components are marked on the plot) together with the RV curve representing the orbit. In the RV curves, squares denote the primary component, triangles denote the secondary component, while the full and dashed lines plot

TABLE 1
BASIC PARAMETERS OF OBSERVED MULTIPLE SYSTEMS

WDS (J2000)	Comp.	HIP	HD	Spectral type	V (mag)	$V-K$ (mag)	μ_α^* (mas yr^{-1})	μ_δ	RV (km s^{-1})	$\overline{\omega}^{\mathrm{a}}$ (mas)
00363−3818	AB	2863	3365	G2/G3V	8.36	1.54	247	−35	−7.07	9.56
01037−3024	AB	4974	6307	F5/6V	8.78	1.20	35	−34	−2.04	13.87[b]
01477−4358	AB	8353	11057	F6/7V	7.97	1.34	52	−7	21.04	5.3[b]
06048−4828	A	28796	41824	G5V	6.57	1.75	−101	−23	21.35	32.51
	B	...	...	...	7.69	...	−117	−39	14.45	32.47
07171−1202	AB	35261	56593	F4V	6.71	1.14	24	−55	−9.0	21.6[b]
07171−1202	C	...	...	...	9.44	2.04	42	−36	−6.49	19.03
18560−2503	A	92929	175345	G0V	7.38	1.42	38	51	0.16	24.20
	B	...	...	...	12.92	...	32	48	...	22.97
23208−5018	AB	115272	220003	F5m	6.05	0.94	45	−72	13.55	13.36
	C	115269	220002	G4IV	8.86	1.40	43	−73	14.30	13.28
23244+1429	AB	115552	220541	F8V	7.60	1.30	17	−17	16.73	6.14
23509−7954	A	117596	223537	G3V	8.02	1.56	−84	5	23.51	18.22
	B	...	...	...	15.55	4.70	−86	8	...	18.11

[a]Proper motions and parallaxes are taken from the *Gaia* DR2 (Gaia collaboration 2018), where available.
[b]*Hipparcos* parallax (van Leeuwen 2007).

TABLE 2
CCF PARAMETERS

HIP	Comp.	N	a	σ (km s^{-1})	$a\sigma$ (km s^{-1})	$V\sin i$ (km s^{-1})	Li 6708Å
2863	B	10	0.127	3.841	0.443	1.3	N
2863	Aa	10	0.116	8.412	0.976	13.8	N
4974	A	11	0.109	4.84	0.528	6.2	Y
4974	Ba	11	0.080	5.79	0.465	8.4	N
4974	Bb	11	0.030	3.67	0.111	2.5	N
8353	Aa	9	0.050	11.97	0.598	20.7	N
8353	B	9	0.093	5.56	0.518	7.9	N
28796	Aa	3	0.325	5.94	1.930	8.8	N
28796	B	4	0.473	3.79	1.795	3.0	N
35261	Ca	11	0.418	3.66	1.53	2.4	N
35261	Cb	11	0.034	5.39	0.184	7.5:	N
92929	Aa	5	0.345	3.68	1.268	2.5	Y
115272	Aa	12	0.071	21.09	1.494	38:	N
115272	B	12	0.029	3.33	0.097	0	N
115272	C	4	0.390	4.09	1.597	4.1	Y?
115552	Aa	9	0.100	4.70	0.733	5.8	Y
115552	Ab	9	0.120	4.73	0.568	5.9	Y
117596	Aa	10	0.120	6.47	0.779	9.9	N
117596	Ab	10	0.103	6.03	0.619	9.0	N

TABLE 3
SPECTROSCOPIC ORBITS

HIP	System	P (d)	T (+24 00000)	e	ω_A (deg)	K_1 (km s^{-1})	K_2 (km s^{-1})	γ (km s^{-1})	rms$_{1,2}$ (km s^{-1})	$M_{1,2}\sin^3 i$ ($\mathcal{M}_\odot$)
HIP 2863	Aa,Ab	4.81156	58377.7635	0.0	0.0	55.124	88.39	−7.058	0.17	0.91
		±0.00005	±0.0008	fixed	fixed	±0.049	±0.55	±0.036	2.23	0.56
HIP 4974	Ba,Bb	14.7104	58385.5078	0.427	114.6	53.318	70.971	−2.043	0.12	1.23
		±0.0002	±0.0086	±0.001	±0.3	±0.137	±0.194	±0.056	0.21	0.93
HIP 8353	Aa,Ab	5.3093	58371.8164	0.000	0.0	56.721	...	21.043	0.83	1.6:
		±0.0001	±0.0042	fixed	fixed	±0.260	...	±0.189	...	>0.86
HIP 28796	Aa,Ab	2.5144	58308.9570	0.038	119.9	17.140	...	21.351	0.36	1.0:
		±0.0000	±0.1716	±0.011	±24.2	±0.370	...	±0.161	...	>0.11
HIP 35261	Ca,Cb	22.49302	58421.602	0.2886	107.36	36.656	49.285	−6.490	0.01	0.74
		±0.00005	±0.003	±0.0002	±0.05	±0.011	±0.400	±0.006	0.73	0.56
HIP 92929	Aa,Ab	312.279	50319.39	0.705	254.1	16.007	...	0.163	0.05	1.1:
		±0.039	±0.40	±0.007	±0.8	±0.299	...	±0.055	...	>0.50
HIP 115272	Aa,Ab	3.42691	58382.8343	0.000	0.0	50.545	...	13.582	0.74	1.8:
		±0.00001	±0.0046	fixed	fixed	±0.488	...	±0.294	...	>0.65
HIP 115552	Aa,Ab	17.4779	58335.2617	0.233	8.0	60.458	62.927	16.727	0.07	1.59
		±0.0003	±0.0184	±0.001	±0.3	±0.068	±0.086	±0.037	0.11	1.53
HIP 117596	Aa,Ab	4.3703	58022.1172	0.000	0.0	73.021	78.103	23.512	0.10	0.81
		±0.0000	±0.0005	fixed	fixed	±0.050	±0.050	±0.025	0.11	0.75

TABLE 4
RADIAL VELOCITIES AND RESIDUALS (FRAGMENT)

HIP	System	Date	RV	σ	(O−C)	Comp.
		(JD +2400000)		(km s^{-1})		
2863	Aa,Ab	57985.7850	−60.88	0.10	0.04	a
2863	Aa,Ab	57985.7850	81.27	1.00	1.96	b
2863	Aa,Ab	58341.8440	−61.16	0.10	−0.28	a
2863	Aa,Ab	58341.8440	81.50	1.00	2.27	b
2863	Aa,Ab	58358.7530	45.30	0.10	−0.16	a
2863	Aa,Ab	58380.8120	−43.96	0.10	−0.05	a
2863	Aa,Ab	58380.8120	50.48	1.00	−1.54	b

TABLE 5
RADIAL VELOCITIES OF OTHER COMPONENTS

| HIP	Comp.	Date	RV
		(JD −2400000)	(km s^{-1})
2863	B	57985.7849	-3.92
2863	B	58341.8436	-3.94
2863	B	58358.7535	-3.86
2863	B	58380.8115	-3.96
2863	B	58382.6616	-3.92
2863	B	58384.6394	-3.98
2863	B	58390.7608	-3.79
2863	B	58393.6771	-3.75
2863	B	58397.6459	-3.94
4974	A	57985.7901	-2.92
4974	A	57986.8340	-2.95
4974	A	58358.7681	-2.92
4974	A	58370.8620	-2.94
4974	A	58380.8179	-3.03
4974	A	58382.6662	-2.84
4974	A	58383.8077	-2.75
4974	A	58384.6054	-2.90
4974	A	58385.8176	-2.88
4974	A	58393.6137	-2.90
8353	B	57985.7997	21.95
8353	B	57986.8466	22.36
8353	B	58370.8769	22.66
8353	B	58380.8455	21.54
8353	B	58382.8260	22.28
8353	B	58384.6274	22.27
8353	B	58385.6427	22.34
8353	B	58393.7654	22.22
28796	B	57266.8736	14.39
28796	B	57319.6842	14.43
28796	B	57364.6872	14.43
28796	B	57374.6120	14.45
28796	B	57985.8975	14.44
28796	B	57986.9151	14.48
28796	B	58193.4814	14.29
28796	B	58195.4857	14.53
28796	B	58382.8844	14.48
28796	B	58395.8906	14.53
28796	B	58407.8409	14.13
28796	B	58408.7916	14.47
28796	B	58409.8807	14.50
115272	B	57984.7192	11.89
115272	B	57986.6695	11.42
115272	B	58340.7511	12.56
115272	B	58341.8367	12.33
115272	B	58342.7908	12.59
115272	B	58356.6185	11.15
115272	B	58380.7650	11.23
115272	B	58382.6583	11.77
115272	B	58383.6587	12.08
115272	B	58384.6362	12.14
115272	B	58385.6255	11.46
115272	B	58390.6450	11.48
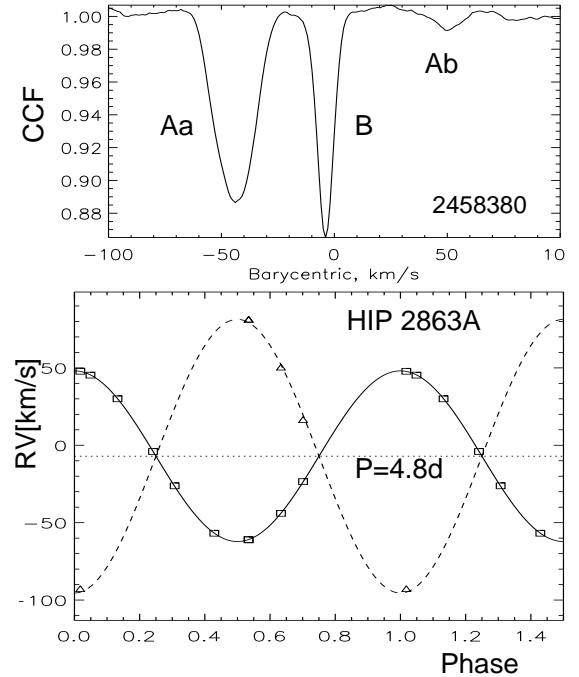
FIG. 1.— CCF (top) and RV curve (bottom) of HIP 2863 Aa,Ab. In this and the following Figures, the upper panel shows a typical CCF, with the date of observation indicated. The lower panel presents the phased RV curve where the full line and squares denote the orbit and RVs of the primary component, the dashed line and triangles refer to the secondary component.

the orbit. Masses of stars are estimated from absolute magnitudes, orbital periods of wide pairs from their projected separations (see Tokovinin 2018a).

3.1. HIP 2863 (Triple)

The 0″.4 visual binary RST 5183 with fast proper motion (PM) was discovered by R.A. Rossiter in 1945. Since then, it moved by 12° in angle and opened up to 0″.7 separation. The orbital period of this pair is estimated at ~400 years.

Nordström et al. (2004) found a large RV variation and double lines. Observations with CHIRON conducted since 2017 show a superposition of two spectra, one with narrow lines and a constant RV of −3.85 km s^{-1} (rms scatter 0.08 km s^{-1}), another with a fast RV variation and wider lines. The latter belongs to the bright component A of the visual binary. Its orbit with a period of 4.8 days is circular (Figure 1). The center-of-mass velocity, −7.07 km s^{-1}, differs from the RV of B owing to the motion in the visual orbit.

Some (but not all) CCFs contain a very weak dip corresponding to Ab, originally ignored. Fitting this dip defines the RV amplitude of Ab and the mass ratio $q_{Aa,Ab} = 0.62$. The mass of Aa deduced from its absolute V magnitude is about 1.3 $M_\odot$, hence the mass of Ab is 0.82 $M_\odot$. Comparison with $M \sin^3 i$ leads to the orbital inclination $i_{Aa,Ab} = 62°$. The mass of B is intermediate, 0.95 $M_\odot$. Slow axial rotation of B and the absence of lithium in the spectrum indicate an old age, in harmony with the fast PM and the metallicity of [Fe/H]=−0.37 (Nordström et al. 2004).

3.2. HIP 4974 (Triple)

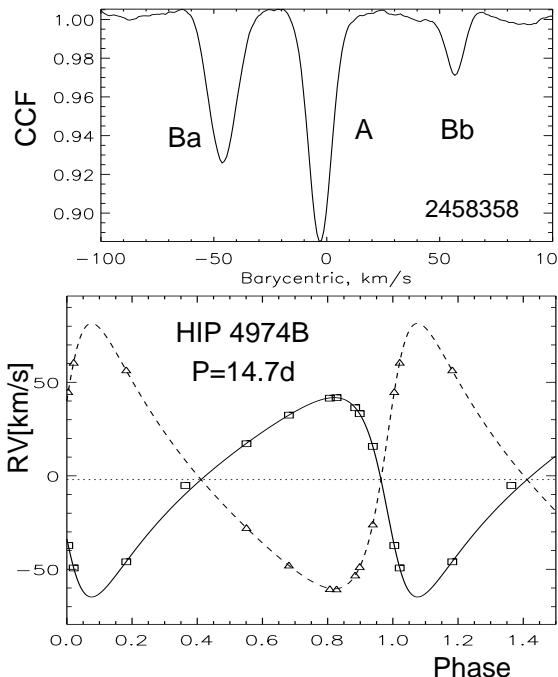Like the previous object, this is a classical visual binary B 649, known since 1927. The orbital separation of 0″.8

FIG. 2.— CCF (top) and RV curve (bottom) of HIP 4974.

FIG. 3.— CCF (top) and RV curve (bottom) of HIP 8353.

corresponds to the period of ∼250 years; the stars are of similar brightness, $\Delta V_{AB} = 0.40$ mag. Only a small arc of the outer orbit is observed. The *Gaia* DR2 parallaxes of A and B are discordant, 5.14±0.46 and 16.09±1.09 mas respectively. The large parallax errors indicate a problem in the data reduction, presumably caused by the small separation. The *Hipparcos* parallax of AB, 13.87 mas, is adopted here. However, it places the unresolved star below the main sequence, so the actual parallax is likely smaller.

The large RV variation reported by Nordström et al. (2004) prompted observations of this system with CHIRON. Independently, eclipses with a period of 14.7104 days and a depth of 0.22 mag were discovered by Otero & Dubovsky (2004). The variable star designation is SI Scl.

The spectrum is triple-lined (Figure 2). The stronger lines, attributed here to the the visual component A, are stationary, with an RV of -2.9 km s^{-1}. They are accompanied by the rapidly moving lines of the subsystem Ba,Bb. Its spectroscopic period, determined independently, matches perfectly the photometric period. The orbit has an eccentricity of 0.43, while the mass ratio $q_{Ba,Bb} = 0.75$. Considering the uncertain distance, estimates of masses from luminosity are questionable. However, the presence of eclipses implies that the spectroscopic masses of Ba and Bb, 1.23 and 0.93 $M_\odot$, are close to the actual masses. A joint analysis of the light curve and RVs will lead to the accurate mass measurement for the eclipsing pair. The presence of lithium in the spectrum of component A and the spatial velocity $(U, V, W) = (-3.4, -17.2, -10.7)$ km s^{-1} (the U axis is directed away from the Galactic center) indicate that this multiple system is relatively young.

It is not certain that the inner subsystem belongs to the visual secondary B. The sum of the CCF areas of Ba and Bb is larger than the area of A by 9%. However, for the spectral type around F5V the CCF area depends on the effective temperature, being larger for
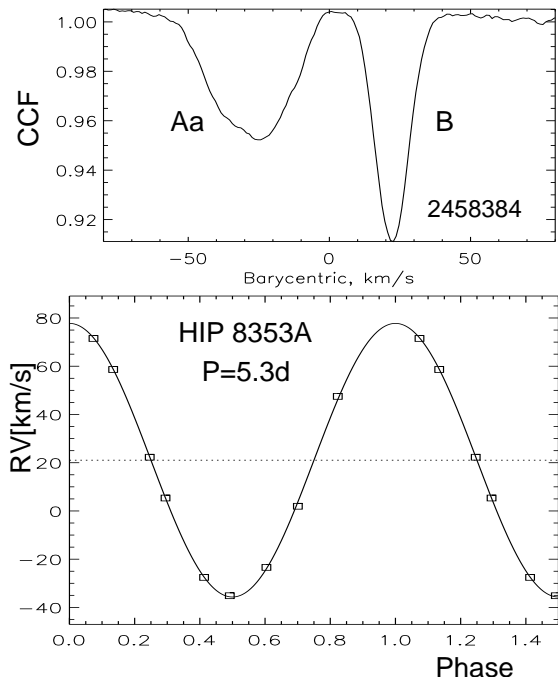
cooler stars. Direct differential photometry of A and B during eclipses or displacement of the photo-center of the unresolved images of AB can confirm the attribution of the spectroscopic pair to the component B.

3.3. *HIP 8353 (Triple)*

This object is a close visual binary I 52 for which a preliminary orbit with $P = 224$ years, a semimajor axis of 0″.372, and a large eccentricity of 0.847 has been computed by Gomez et al. (2016). The components A and B are similar, $\Delta V_{AB} \approx 0.5$ mag. Owing to the resolved nature of the source, *Gaia* does not yet provide the parallax, and I adopt the original *Hipparcos* parallax of 5.3±1.2 mas. The estimated mass sum and the visual orbit correspond to the dynamical parallax of 6.4 mas.

As noted by Nordström et al. (2004), the spectrum is double-lined. I attribute the narrow stationary lines to the visual component B and the wider moving lines to the component Aa, although this choice is not absolutely certain. The mean RV of B is 22.15 km s^{-1} with rms scatter of 0.28 km s^{-1}. The circular orbit of Aa,Ab with a period of 5.3 days is computed here (Figure 3). Large residuals of 0.83 km s^{-1} are explained by the wide and shallow dip of Aa, probably distorted by star-spots. If the masses of Aa and B are 1.67 and 1.50 $M_\odot$, as deduced from their absolute magnitudes, the minimum mass of Ab is 0.81 $M_\odot$. As its lines are not detectable, it could be either a low-mass dwarf or a cold white dwarf. The Vizier photometry tool[3] does not indicate any ultraviolet excess.

3.4. *HIP 28796 (Triple)*

This is a nearby (distance 30.7 pc) chromospherically active triple system V575 Pup (HR 2162). Activity and X-ray flux suggest a young age, and membership in the Castor moving group was proposed by Caballero (2010).
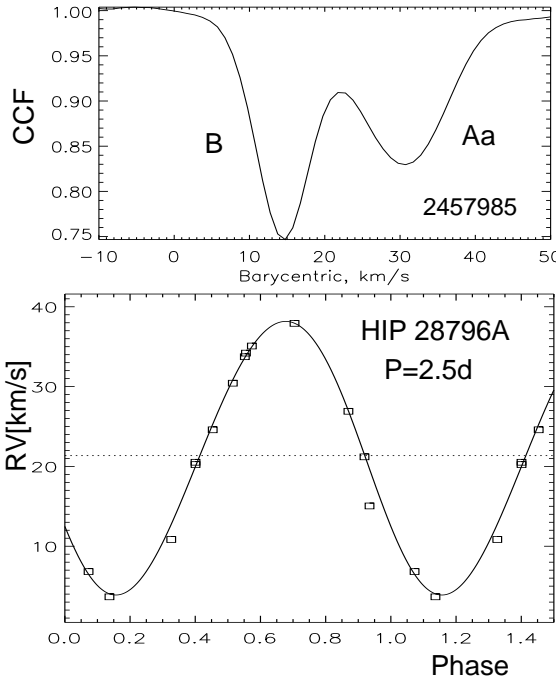
---

[3] See http://vizier.u-strasbg.fr/vizier/sed/

FIG. 4.— CCF (top) and RV curve (bottom) of HIP 28796.

FIG. 5.— CCF (top) and RV curve (bottom) of HIP 35261C.

However, the spatial velocity of HIP 28796 $(U, V, W) = (-2.5, -11.7, -23.2)$ is quite distinct from the motion of that group. Plavchan et al. (2009) searched for excess thermal emission from a debris disk but have not found any.

The visual orbit of the outer pair A,B is uncertain; the latest one (Tokovinin et al. 2014) has the period of 916 years and the semimajor axis of $4''.578$. The large RV variability detected by Nordström et al. (2004) implied the existence of a spectroscopic subsystem. Its orbit determined here has a period of 2.51 days (Figure 4). Interestingly, the eccentricity is marginally significant ($e = 0.038 \pm 0.011$), despite the short period. The visual binary has currently a separation of $2''.6$, allowing to differentiate the light of components in the CHIRON fiber under good seeing. Several resolved spectra of both components were taken; in the remaining spectra, the light of A and B is mixed and the CCF has a double dip, as shown in Figure 4.

Synchronous rotation of the star Aa, of one solar radius, corresponds to the equatorial speed of 20 km s^{-1}. Comparison with the projected rotation of 8.8 km s^{-1} provides an estimate of the orbital inclination $i_{\rm Aa,Ab} \approx 26°$. The minimum mass of Ab is 0.11 $M_\odot$; accounting for the inclination, the true mass is about 0.3 $M_\odot$.

Slow axial rotation of the component B and the absence of the lithium line in the spectra suggest that this triple system is relatively old. The fast rotation of Aa and its chromospheric activity are sustained by the angular momentum of the close binary.

The RV of B is constant at 14.45 km s^{-1} with the rms scatter of 0.11 km s^{-1}, while the center-of-mass velocity of Aa,Ab is 21.35 km s^{-1}. The difference RV(B)−RV(A)=−6.9±0.2 km s^{-1} might seem too large for the millennium-long outer period. The orbit was re-fitted to evaluate its reliability, resulting in $P_{\rm A,B} = 947 \pm 289$ years, $a_{\rm A,B} = 4''.48 \pm 0''.76$, and $e_{\rm A,B} =$
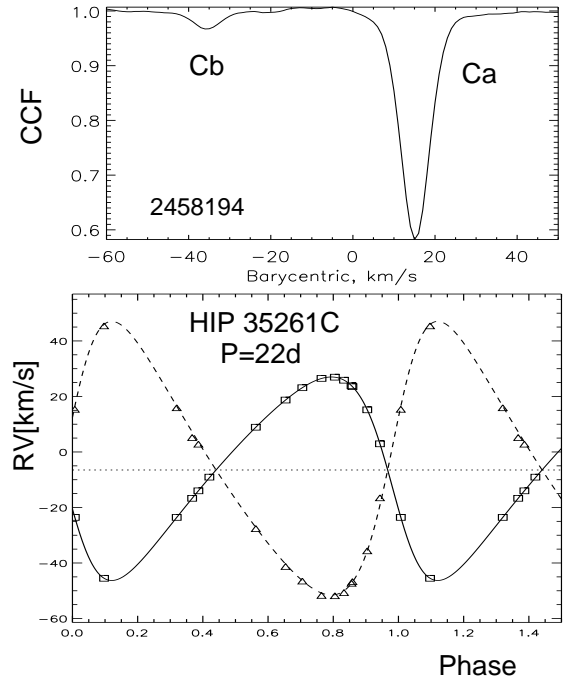
0.43 ± 0.11. The *Gaia* parallaxes of A and B are accurate and mutually consistent, $\overline{\varpi}_{\rm A} = 32.51 \pm 0.03$ mas and $\overline{\varpi}_{\rm B} = 32.47 \pm 0.03$ mas. The average parallax and the still uncertain orbit lead to the mass sum of 3.11 ± 0.19 $M_\odot$, larger than the estimated mass sum of 2.25 $M_\odot$. The pair A,B is presently located near the node of its orbit and the computed RV difference between B and A is -6.1 km s^{-1}, only slightly less than actually measured. The true ascending node of the orbit is $\Omega_{\rm A} = 122°$. The RV of B is constant during three years covered by CHIRON. The observed motion of the pair A,B is smooth, without any hint of astrometric perturbation. Therefore, the existence of additional companions to B is highly unlikely.

3.5. *HIP 35261 (Quadruple)*

This is a nearby (53 pc) quadruple system. The outer $15''.9$ pair STF 1064 AB,C is known since 1831 and is definitely physical. Its main component is the visual binary A 2123 A,B with a known orbit of 80 year period and the semimajor axis of $0''.64$. This pair is not present in the *Gaia* DR2, while its HIP2 parallax is 21.6±2.1 mas. On the other hand, the component C has a well-measured DR2 parallax of 19.03±0.07 mas. Tokovinin (2015) discovered that C is a double-lined binary with very unequal dips. Here I compute its spectroscopic orbit with $P = 22$ days (Figure 5) using RVs measured in 2015–2018. The residuals for the component Ca are only 0.013 km s^{-1}, owing to its narrow and deep spectral lines.

Comparison between spectroscopic and estimated masses of the pair Ca,Cb leads to an orbital inclination of 74°. Interestingly, the inclination of A,B is 78°; the two orbits could be (but not necessarily are) coplanar. The component Ca is, apparently, a normal slowly rotating K1V dwarf. The dip of Cb is so weak that its parameters are poorly measured.
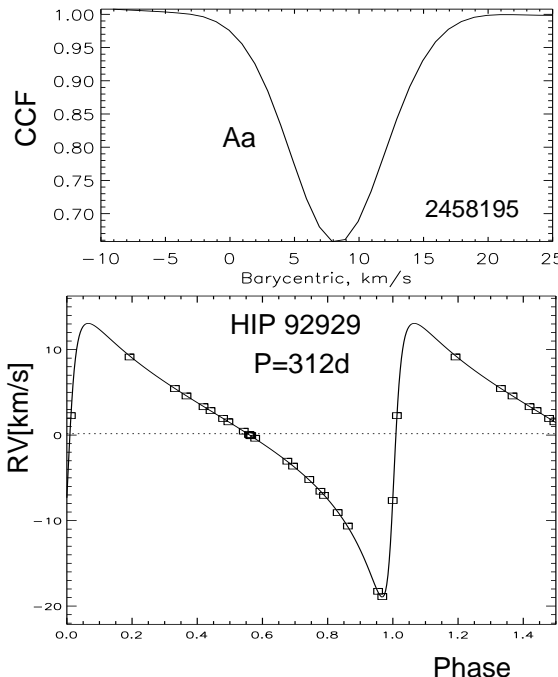
3.6. *HIP 92929 (Triple)*

FIG. 6.— CCF (top) and RV curve (bottom) of HIP 92929.

FIG. 7.— CCF (top) and RV curve (bottom) of HIP 115272. The three RVs measured by Nordstrom & Andersen (1985) are plotted as crosses.

The outer system is a $6\rlap{.}''2$ visual binary B 413 with a large $\Delta V = 5.6$ mag, an estimated period of ~ 3 kyr, and the correspondingly slow relative motion. The RV variation of the brighter component A was noted by Jenkins et al. (2015) during search for exo-planets. They determined a preliminary orbit with $P = 312$ days and $e = 0.75$, although the coverage of the RV curve was incomplete. The period is confirmed by CHIRON observations, but the eccentricity is different, $e = 0.70$; it is well constrained by RVs on the rising branch of the RV curve in Figure 6. Precise RVs from Jenkins et al. (2015) match the CHIRON RVs very well because the orbit computed from the combined data has residuals of only 0.045 km s^{-1}, without any adjustment of the velocity zero point. The minimum mass of the secondary component Ab is 0.5 $M_\odot$.

The narrow CCF dip of Aa has a large depth and corresponds to $V \sin i = 2.5$ km s^{-1}. Despite the slow projected axial rotation, the spectrum contains a strong lithium line with an equivalent width of 38 mÅ. The spatial velocity $(U, V, W) = (-2.7, 11.9, -2.7)$ km s^{-1} does not match any known kinematic group.

3.7. HIP 115272 (Quadruple)

This bright quadruple system is located at 75 pc from the Sun. The outer $17''$ pair AB,C (DUN 248) is composed of HIP 115272 and HIP 115269, with common PMs, parallaxes, and RVs. The period of AB,C is on the order of 20 kyr. The mean RV of the component C measured with CHIRON is 14.301 km s^{-1} with the rms scatter of 0.016 km s^{-1}. At the next hierarchical level we find the $1\rlap{.}''3$ visual binary A,B (RST 5560) with $\Delta V = 2$ mag, an estimated period of ~ 500 years, and unknown orbit. Double lines in the spectrum of this star were noted by Nordström & Andersen (1985), suggesting that it contains an even closer spectroscopic binary.

The CHIRON spectra of AB show double lines. The set of weaker lines is stationary with the mean RV of
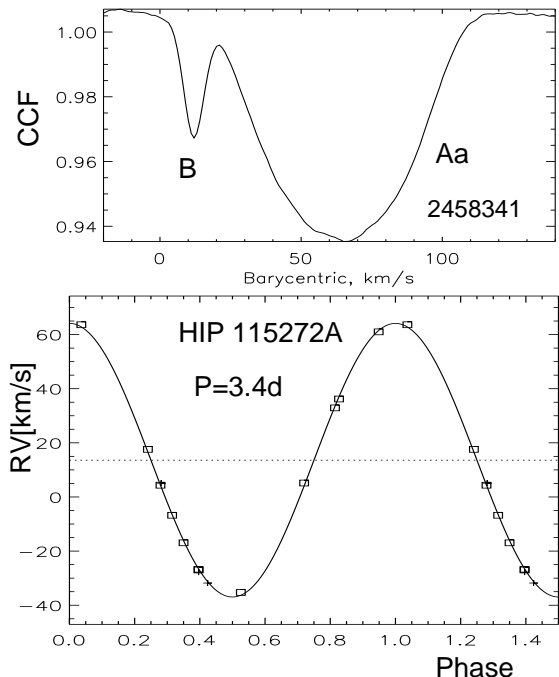
11.94 km s^{-1} (rms scatter 0.47 km s^{-1}); it corresponds to the visual secondary component B. The stronger lines of Aa move with the period of 3.4 days on a circular orbit (Figure 7). The three RVs from Nordström & Andersen (1985) match the orbit and improve the accuracy of the period. The mass of the metallic-line F5m component Aa, estimated crudely from its absolute magnitude, is 1.8 $M_\odot$, hence the minimum mass of Ab is 0.65 $M_\odot$. The component C is located on the main sequence, while AB is above it. With the Aa radius of 2.75 $R_\odot$ estimated by *Gaia*, the synchronous equatorial velocity is 40 km s^{-1}, in rough agreement with the actual width of the CCF dip.

3.8. HIP 115552 (Triple)

This triple system consists of the $1\rlap{.}''5$ visual binary A,B (BU 719, estimated period 1.5 kyr) and the double-lined spectroscopic subsystem Aa,Ab with the period of 17.5 days and a moderately eccentric orbit (Figure 8). The spectroscopic subsystem was discovered by Nordström et al. (2004). The visual secondary B is 3 mag fainter than A and its lines are not detected in the spectra, although the persistent weak detail of the CCFs near the center-of-mass velocity may actually correspond to B.

The two stars Aa and Ab, of F8V spectral type, are nearly equal, the mass ratio is $q_{\rm Aa,Ab} = 0.96$. Their estimated masses are 1.65 $M_\odot$ each, close to the spectroscopic masses $M \sin^3 i$ of 1.6 $M_\odot$. Therefore, the orbital inclination is large, $i_{\rm Aa,Ab} \approx 80°$.

Stellar rotation in a binary with an orbital period of 17.5 days is not expected to be synchronous. Indeed, both Aa and Ab rotate with $V \sin i = 5.8$ km s^{-1}, faster than the pseudo-synchronous speed of 3.8 km s^{-1}, calculated for $1 R_\odot$ radius. The presence of lithium in the spectra of both components points to the young age, as well as their location above the main sequence. These stars are too luminous for their spectral type F8V (which matches
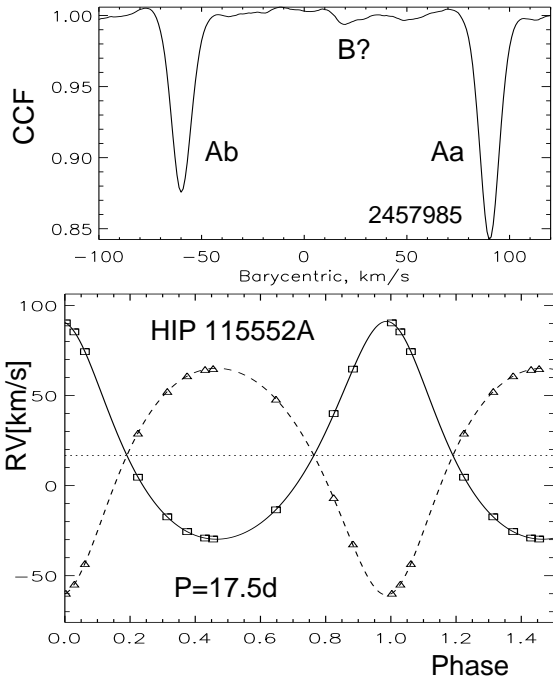
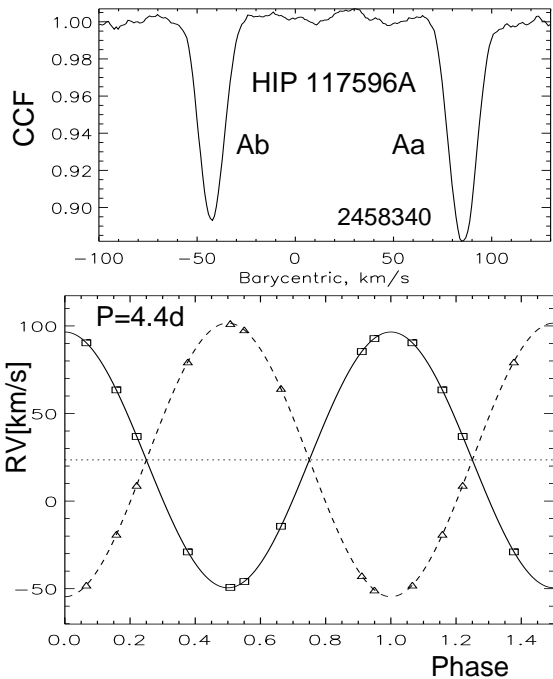FIG. 8.— CCF (top) and RV curve (bottom) of HIP 115552.

FIG. 9.— CCF (top) and RV curve (bottom) of HIP 1117596.

the $V - K$ color) by a factor of ~ 4. However, the spatial velocity $(U, V, W) = (-5.5, -0.1, -24.0)$ km s^{-1} does not match any known group of young stars.

3.9. *HIP 117596 (Triple)*

The outer pair A,B is wide (30.″7, UC 5034). The faint ($V = 15.55$ mag) star B has common PM and parallax with A according to *Gaia* DR2. Its color and luminosity match a dwarf of spectral type M3V. The estimated period of A,B is of the order of 50 kyr. The system is moderately metal-poor, [Fe/H] $= -0.37$ (Nordström et

al. 2004). The absence of lithium indicates that it is not young.

Double lines in the spectrum of A have been noted by Nordström et al. (2004). The system is featured in the catalog of chromospherically active binaries by Eker et al. (2008), although they do not provide the period. The circular orbit of Aa,Ab with $P = 4.37$ days is determined here (Figure 9). This is a twin pair with $q_{\rm Aa,Ab} = 0.93$. The estimated masses of 0.99 and 0.93 solar are close to the spectroscopic masses, hence the inclination is large, $i_{\rm Aa,Ab} \approx 70°$. The synchronous equatorial rotation of ~ 11 km s^{-1} roughly matches the measured $V \sin i$.

4. SUMMARY

Monitoring of hierarchical systems with CHIRON has led to the determination of 23 orbits published in the papers 1–4; the paper 5 brings the total to 32. The cumulative contribution of this program to the data on nearby low-mass hierarchies is far from negligible. For example, the number of spectroscopic subsystems with unknown periods in the 67-pc sample of solar-type stars (Tokovinin 2014) was 61. After excluding long-period (e.g. astrometric) subsystems and the recently determined orbits, the number of unknown short periods before this publication was 13, and four of those are defined here. Complete coverage of the short-period hierarchies in this volume-limited sample can be reached soon. It will establish the unbiased distributions of periods and mass ratios of the inner subsystems that will help to clarify the still debated origin of close binaries. The preference of close binaries to be members of hierarchies is a known fact which may be explained in several different ways (Moe & Kratter 2018).

In this survey-type work I inevitably encounter interesting and unusual systems, such as the young quadruple system HD 86588 with a short period and, yet, eccentric orbit (Tokovinin et al. 2018). Several compact triple systems where both outer and inner spectroscopic orbits can be derived will be presented in the future paper of this series when their outer orbits are covered. Unusual hierarchies give additional clues to the origin of stellar systems.

8

REFERENCES

Caballero, J. A. 2010, A&A, 514, 98
Eker, Z., Filiz Ak, N., Bilir, S. et al. 2008, MNRAS, 389, 1722
Gaia Collaboration, Brown, A. G. A., Vallenari, A., Prusti, T. et al. 2018, A&A, 595A, 2 (Vizier Catalog I/345/gaia2).
Gomez, J., Docobo, J. A., Campo, P. P. & Mendez, R. A. 2016, AJ, 152, 216
Jenkins, J. S., Díaz, M., Jones, H. R. A. et al. 2015, MNRAS, 453, 1439
Mason, B. D., Wycoff, G. L., Hartkopf, W. I., Douglass, G. G. & Worley, C. E. 2001, AJ, 122, 3466 (WDS)
Moe, M. & Kratter, K. M. 2018, ApJ, 854, 44
Nordstrom, B. & Andersen, J. 1985, A&AS, 61, 53
Nordström, B., Mayor, M., Andersen, J. et al. 2004, A&A, 418, 989
Otero, S. A. & Dubovsky, P. A. 2002, IBVS, 5557, 10
Plavchan, P., Werner, M. W., Chen, C. H. et al. 2009, ApJ, 698, 1068
Tokovinin, A. AJ, 2014, 147, 86

Tokovinin, A. 2015, AJ, 150, 177
Tokovinin, A. 2016a, AJ, 152, 11 (Paper 1)
Tokovinin, A. 2016b, AJ, 152, 10 (Paper 2)
Tokovinin, A. 2016c, ORBIT: IDL Software for Visual, Spectroscopic, and Combined Orbits, Zenodo, doi:10.2581/zenodo.61119
Tokovinin, A. 2018a, ApJS, 235, 6
Tokovinin, A. 2018b, AJ, 156, 48 (Paper 3)
Tokovinin, A. 2018c, AJ, 156, 194 (Paper 4)
Tokovinin, A., Fischer, D. A., Bonati, M. et al. 2013, PASP, 125, 1336
Tokovinin, A., Mason, B. D. & Hartkopf, W. I. 2014, AJ, 147, 123
Tokovinin, A., Corbett, H., Fors, O., et al. 2018, AJ, 156, 120
van Leeuwen, F. 2007, A&A, 474, 653 (HIP2)